Picosecond Dynamics of Silver Nanoclusters. Photoejection of Electrons and Fragmentation

Prashant V. Kamat,* Mark Flumiani,† and Gregory V. Hartland‡

Notre Dame Radiation Laboratory and Department of Chemistry, University of Notre Dame, Notre Dame, Indiana 46556-0579

Received: October 28, 1997; In Final Form: February 10, 1998

Silver colloids of particle diameter 40−60 nm have been synthesized using a chemical reduction method in aqueous medium. These nanoclusters are photoactive and exhibit transient bleaching in the 400−500 nm region followed by a strong absorption in the visible−near-infrared region when subjected to 355 nm laser-pulse excitation. The transient bleaching of the surface plasmon absorption band is a monophotonic process, while the absorption growth in the red region is a biphotonic process arising from the photoejection of electrons. The 40−60 nm clusters were observed to break up into smaller clusters (5−20 nm) with 355 nm laser-pulse excitation. The choice of excitation wavelength provides the size selectivity in the fragmentation of the clusters. For example, when the excitation wavelength was switched to 532 nm, only larger (or irregularly shaped) particles were found to break up.

Introduction

Although metal colloids have been known for over a hundred years, it is only recently that attention has been focused on understanding their photocatalytic properties. Some similarities exist between metal and semiconductor nanoclusters with respect to their photophysical properties.[1,2] They are optically transparent and act as dipoles. They are also photoactive and participate in catalytic reactions. On the other hand, noble metals in bulk are only photoactive to a small extent, although photoelectron emission from silver electrodes has been noted by Gerischer and co-workers.[3] The nanoparticles of these materials exhibit excellent photochemical activity because of their high surface/volume ratio and unusual electronic properties. For example, Henglein and co-workers[4,5] reported photochemical dissolution of Ag colloids when photoejected electrons were scavenged by species such as N_2O.

Although the conduction and valence bands of semiconductors are separated by a well-defined band gap, metal nanoclusters have close-lying bands and electrons move quite freely. The free electrons give rise to a surface plasmon absorption band in metal clusters, which depends on both the cluster size and chemical surroundings.[1,6,7] The surface plasmon band is sensitive to laser excitation. For example, the surface plasmon band of gold particles is bleached on a subpicosecond time scale when excited with a UV or visible laser pulse. The electron dynamics of Au and Ag nanoclusters have recently been investigated by picosecond transient grating spectroscopy[8] and femtosecond transient absorption spectroscopy.[9−13] These photophysical investigations primarily demonstrated how the electronic excitation in metal particles is coupled to phonon modes.

Significant efforts have been made in our laboratories and elsewhere to investigate the photophysical and photochemical behavior of single and multicomponent metals and semiconductor nanoclusters.[6,14−23] Such composite materials are especially of interest in developing efficient light-energy conversion systems, optical devices, and microelectronics. For example, photoinduced deposition of noble metals such as Pt or Au on semiconductor nanoclusters has often been employed to enhance their photocatalytic activity.[24,25] In our continued efforts to explore the optical properties of various nanoclusters, we have now elucidated the photochemical response of silver nanoclusters to UV and visible laser excitations. The picosecond−nanosecond events leading to the fragmentation of 40−60 nm diameter silver clusters are presented here.

Experimental Section

Ag colloids were prepared by the conventional reduction method of reducing $AgNO_3$ (0.12 mM) in water with sodium citrate at near-boiling temperature.[26] The concentration of sodium citrate employed for the reduction was kept low (0.42 mM) to avoid the presence of excess citric acid in the silver suspension. For transmission electron microscopic examination of colloids, a drop of the colloid sample was applied to a carbon-coated copper grid. Particle sizes were determined from the photographs taken at a magnification of 150000× using a Hitachi H600 transmission electron microscope. The pictures were further magnified by photographic enlargement.

Absorption spectra were recorded with a Milton Roy 3000 diode array spectrophotometer. UV photolysis was performed with a filtered light (λ > 300 nm) from a 250 W xenon lamp. Steady-state γ radiolysis was carried out with a ^{60}Co source. (Dose rate ≈ 53 Gy min^{-1}). Picosecond laser flash photolysis experiments were performed with 355 or 532 nm laser pulses from a mode-locked, Q-switched Continuum YG-501 DP Nd:YAG laser system (output 2−3 mJ/pulse, pulse width of ∼18 ps). The white continuum picosecond probe pulse was generated by passing the fundamental output through a D_2O/H_2O solution. The pump laser was focused (2 mm × 10 mm) on the sample cell and the experiments were carried out with a right-angle pump/probe geometry. The colloidal suspension was deaerated with N_2 and flowed continuously through the sample cell. The details of the experimental setup and its operation are described elsewhere.[27,28]

Nanosecond laser flash photolysis experiments were per-

* Address correspondence to this author at Notre Dame Radiation Laboratory. E-mail: Kamat.1@nd.edu or http://www.nd.edu/∼pkamat.
† Co-op student from Department of Chemistry, University of Waterloo.
‡ Department of Chemistry. E-mail: Hartland.1@nd.edu.

S1089-5647(98)00009-1 CCC: $15.00
Published on Web 04/07/1998

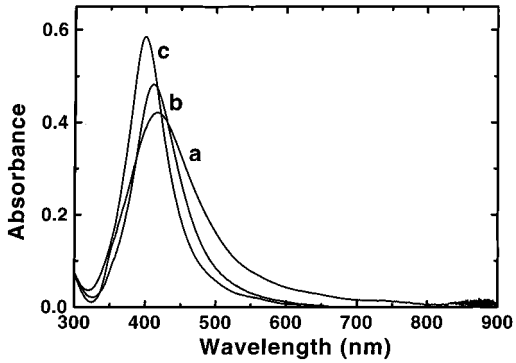

Figure 1. Absorption spectra of 3.0×10^{-4} M colloidal Ag in water (2 mm path length cell): (a) before photolysis, (b) after 2 h of steady-state excitation using xenon lamp ($\lambda > 300$ nm), and (c) after 355 nm laser-pulse excitation (1.5 mJ, 10 Hz) for 3 min.

formed with a Quanta Ray model CDR-1 Nd:YAG system using the 355 nm (third harmonic) laser pulse (~6 ns laser width) for excitation.[29] The laser output was suitably attenuated to less than 10 mJ/pulse and defocused to cover a circular area of ~5 mm in diameter. The experiments were performed in a rectangular quartz cell of 6 mm path length with a right-angle configuration between the directions of laser excitation and analyzing light. The photomultiplier output was digitized with a Tektronix 7912 AD programmable digitizer. A typical experiment consisted of a series of five replicate shots/single measurement.

Results

Silver Colloids. The citrate reduction method produces relatively larger-sized silver nanoparticles with diameters ranging from 40 to 60 nm. The absorption spectrum (spectrum a in Figure 1) of the silver colloids shows a surface plasmon absorption band with a maximum around 420 nm. This absorption band is rather broad and red-shifted compared with the plasmon absorption band of silver colloids prepared by radiolysis and other reduction methods.[5,30−32] As discussed earlier,[1,6,7,33] the position and shape of the plasmon absorption of silver nanoclusters are strongly dependent on the particle size, dielectric medium, and surface-adsorbed species. The transmission electron micrographs of silver nanoclusters synthesized by the citrate reduction method are shown in Figure 2A. The silver particles in these samples exhibit a wide dispersity in particle size and shape. A few faceted nanocrystals can also be seen from the electron micrograph.

The 355 nm laser-pulse excitation of these silver nanoclusters led to some interesting changes in the absorption spectrum (spectrum c in Figure 1). The silver colloid suspension exhibited a blue shift in the absorption maximum when irradiated with 355 nm laser pulses (1.5 mJ, 10 Hz frequency) for 3 min. The blue shift in the absorption maximum was accompanied by a narrowing of the surface plasmon band and an increase in the magnitude of absorption. A similar effect could also be noted upon irradiating the Ag colloid suspension with UV light from a xenon lamp for 2 h. Compared to laser excitation, steady-state photolysis produced relatively small changes (spectrum b in Figure 1). The shift in the plasmon absorption was permanent and did not recover upon stopping the illumination. The blue shift and increase in the oscillator strength of the surface plasmon band is indicative of a decrease in particle diameter. One possibility is that the relatively large (40−60 nm) silver particles employed in the present study become charged when subjected to laser-pulse excitation. Once these clusters accumulate sufficient charge, they may break up to form smaller clusters.

If indeed this hypothesis is true, we should be able to observe these changes in the transmission electron micrograph. We recorded the transmission electron micrographs of silver colloids before and after 355 nm laser-pulse excitation. The electron micrograph shown in Figure 2B confirms that the silver particles in the photolyzed sample are significantly smaller (3−5 times) than the ones in unphotolyzed samples. These silver nanoclusters are also polydisperse with particle diameters of 5−20 nm. The effect of charging on the larger Ag clusters was checked by reacting the Ag nanoclusters with aqueous electrons in steady-state γ radiolysis experiments. The absorption maximum of the Ag nanoparticles exhibited a blue shift upon γ radiolysis for 15 min, a trend similar to that observed in the laser photolysis experiments. Note that complementary photochemical reactivity of Ag nanoclusters was observed in the steady-state photolysis experiments by Linnert et al.[5] These researchers observed dissolution of Ag nanoclusters when irradiated with UV light and in the presence of an electron scavenger. Although some dissolution of Ag is a possibility in the present experiments, the major photochemical event seems to be the breakup of larger particles.

Transient Photobleaching of Silver Nanoclusters. The photophysical properties of silver colloids were further probed by performing time-resolved transient absorption experiments in a picosecond laser flash photolysis apparatus. Transient absorption spectra recorded at different delay times following 355 nm laser-pulse excitation (18 ps pulse width) are shown in Figure 3. The difference absorption spectrum of silver nanoclusters recorded immediately after the laser-pulse excitation shows an intense bleaching of the surface plasmon band at 420 nm. This behavior is very similar to the surface plasmon bleach observed in the case of Au nanoclusters.[10] The plasmon band of metal particles as explained on the basis of Mie theory involves dipolar oscillations of the free electrons in the

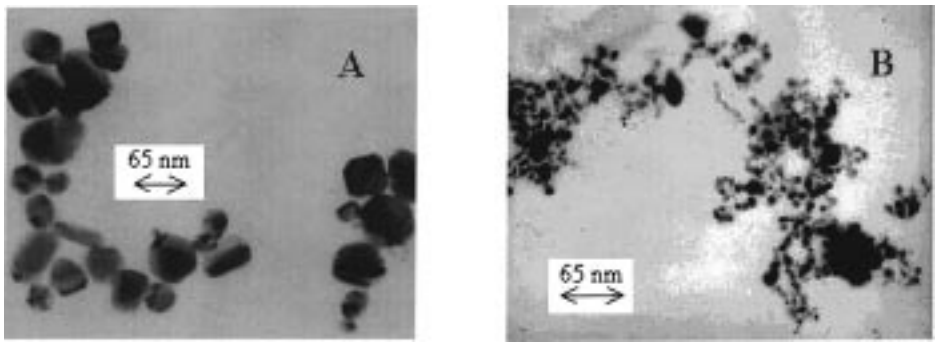

Figure 2. Tunneling electron micrographs (TEM) recorded with a magnification of 150000×: (A) Ag colloids prepared with citric acid reduction method and (B) same colloidal suspension after photolysis with 355 nm (1.5 mJ, 10 Hz) laser excitation for 3 min.

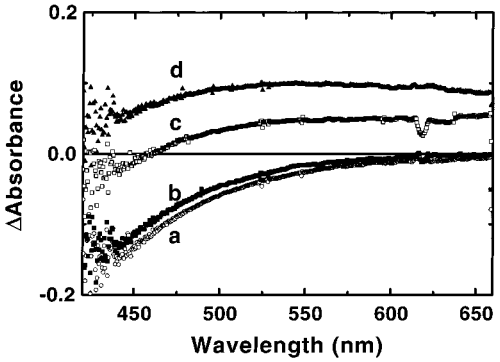

Figure 3. Time-resolved difference absorption spectra of 5.1×10^{-4} M colloidal Ag suspension in water (deaerated) (355 nm laser-pulse excitation, 1.4 mJ). The transient spectra were recorded at delay times of (a) 250, (b) 500, (c) 1250, and (d) 2500 ps.

conduction band that occupy energy states near the Fermi level.[6,34] Once these electrons are excited by a laser pulse, they do not oscillate at the same frequency as that of the unexcited electrons, thus causing the plasmon absorption band to bleach. These aspects have been addressed in several recent spectroscopic investigations.[8,10]

The surface plasmon absorption band of metal nanoclusters is very sensitive to the surface-adsorbed species and dielectric of the medium. For example, chemisorbed I^-, SH^-, and $C_6H_5S^-$ ions result in damping of the surface plasmon band of colloidal silver particles.[35,36] Alternatively, one can also observe bleaching of the surface plasmon band with electrons deposited from radiolytically produced radicals, which cause a blue shift and narrowing of the plasmon band.[37] A more detailed discussion on the damping effects caused by surrounding material can be found elsewhere.[6,7,38]

Recovery and Growth Kinetics. It is evident from Figure 3 that the surface plasmon bleaching recovers quickly and this is followed by an absorption growth in the red region of the spectrum. We monitored these two processes separately by recording the absorption−time profiles at 440 and 600, respectively (Figure 4). The 440 nm trace was analyzed with a double-exponential kinetic fit, which gave time constants of 90 ps and 1.37 ns, respectively. The absorption growth monitored at 600 nm was fitted to a single-exponential growth kinetics with a lifetime of 1.5 ± 0.1 ns. This lifetime is similar to the value (1.37 ns) obtained from the slower component of the 440 nm bleach recovery trace.

Laser-Intensity Dependence. The transient bleaching (Figure 5) and the absorption growth in the red region (Figure 6) was monitored as a function of laser-excitation intensity. Neutral density filters were introduced into the path of the excitation pulse to modulate the excitation intensity. Both the surface plasmon bleach at short times and the broad absorption at longer times (3 ns) increases with increasing laser intensity, but with a different relationship. At intensities less than 1 mJ/pulse, the plasmon bleach increases linearly with the laser intensity, thereby indicating that the bleaching is a monophotonic process. The plasmon bleach becomes independent of laser power at higher intensity owing to saturation of the absorption transition. The long-term absorption in the visible and red regions of the spectrum, on the other hand, deviates from the linear dose dependence. The 600 nm absorption monitored 3 ns after laser-pulse excitation exhibits a quadratic dependence on the laser dose. This laser-power dependence confirms the origin of the broad absorbance in the red as being biphotonic. In other words, the primary electron ejection event needs two 355 nm photons. Although many such electron ejection/electron trapping events are necessary to break up a silver nanocluster, the primary process is biphotonic, which yields a quadratic power dependence.

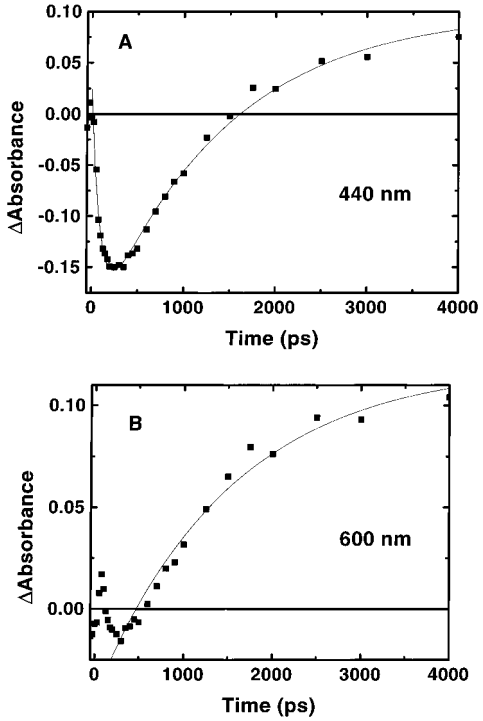

Figure 4. Growth and recovery kinetics of the transients generated following the 355 nm laser-pulse excitation of 5.1×10^{-4} M colloidal Ag suspension in water (deaerated). The monitoring wavelengths were (A) 440 nm and (B) 600 nm.

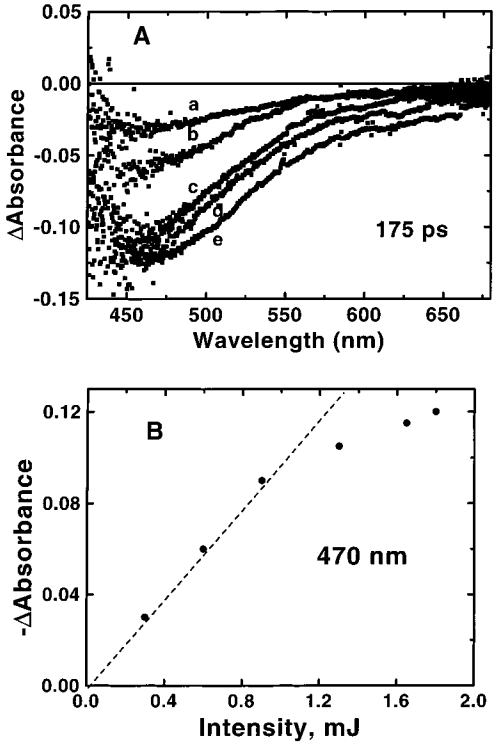

Figure 5. Intensity dependence of surface plasmon bleach recorded from the transient spectra at 175 ps delay. A 1.3×10^{-4} M colloidal Ag suspension in water (deaerated) was excited with 355 nm laser-pulse excitation at various intensity levels. (A) Transient spectra were recorded at excitation intensities of (a) 0.3, (b) 0.6, (c) 0.9, (d) 1.3, and (e) 1.9 mJ. (B) Dependence of maximum bleach at 470 nm on the laser-pulse intensity is shown.

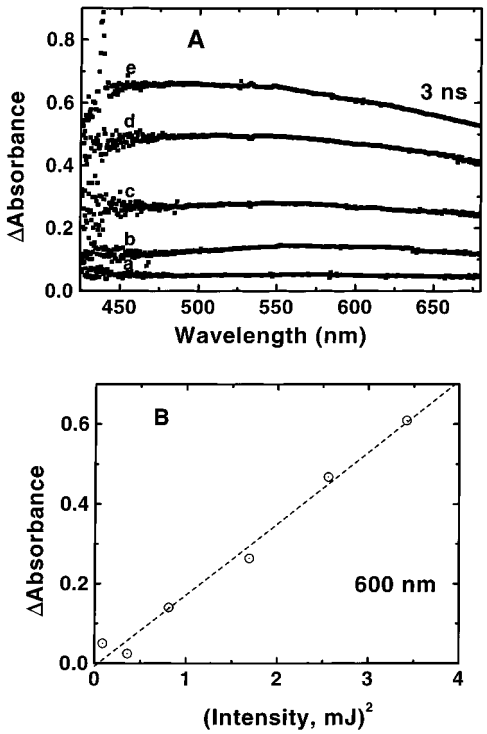

Figure 6. Intensity dependence of the long-lived transient absorption recorded from the transient spectra at 3 ns delay. A 1.3×10^{-4} M colloidal Ag suspension in water (deaerated) was excited with 355 nm laser-pulse excitation at different intensity levels. (A) Transient spectra were recorded at different laser excitation intensities of (a) 0.3, (b) 0.9, (c) 1.3, (d) 1.6, and (e) 1.9 mJ. (B) Dependence of maximum absorbance at 600 nm on the laser-pulse intensity.

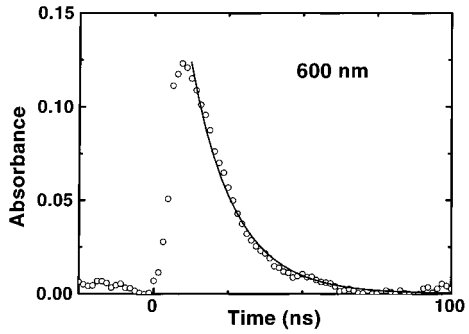

Figure 7. Long-term decay of the transient at 600 nm. A 1.3×10^{-4} M colloidal Ag suspension in water (deaerated) was excited with 355 nm laser-pulse excitation (pulse width of 6 ns) in a nanosecond laser flash photolysis set up.

To further examine the decay of the transient absorption at 600 nm, we extended our study using nanosecond laser flash photolysis. The transient decay monitored at 600 nm following 355 nm laser-pulse excitation (pulse width 6 ns) is shown in Figure 7. Almost complete decay of the 600 nm absorption is seen within the time period of 100 ns. An exponential decay fit of this trace yields a lifetime of 14.2 ± 1 ns. A corresponding increase in the absorption was also observed at 390 nm. Because of the interference from the scattered laser pulse, we were not able to resolve the growth component precisely.

Picosecond Dynamics with 532 nm Excitation. The broad nature of the plasmon band in the present experiments is indicative of a wide range of particle sizes and shapes. Almost all the different size/shape particles absorb incident light when they are subjected to 355 nm laser excitation. This is evidenced by the transient photobleach (Figure 3, spectrum a), which has spectral features that nearly mirror the ground-state spectrum.

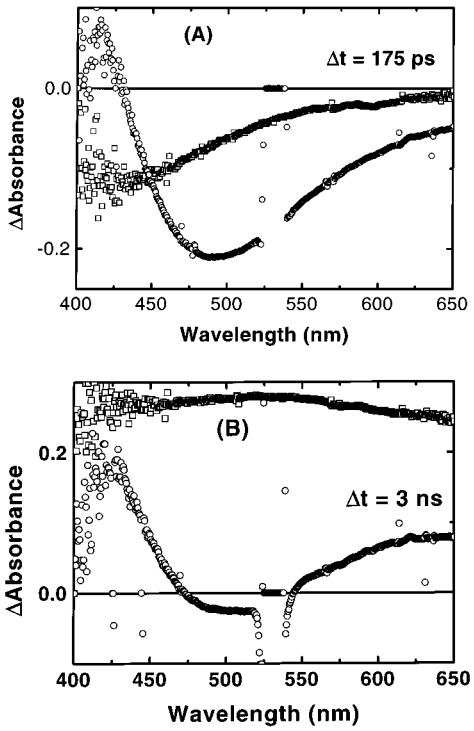

Figure 8. Difference absorption spectra of 5.1×10^{-4} M colloidal Ag suspension in water (deaerated) recorded in a picosecond laser flash photolysis apparatus. The spectra were recorded at delay times of (A) 175 ps and (B) 3 ns using (a) 355 nm and (b) 532 nm laser pulse as the excitation source (pump).

However, by changing the excitation wavelength, we should be able to selectively excite particles within a range of sizes and/or shapes. For example, if we carry out the excitation at a longer wavelength, we expect excitation of those silver clusters that do not contribute to the main plasmon band. Such a particle-geometry-selective excitation strategy has already been used to photodissolve Ag and CdS nanoclusters with steady-state monochromatic irradiation.[5,31,39] We performed these long-wavelength excitation experiments using 532 nm laser pulses. Parts A and B of Figure 8 show the transient spectra recorded at 175 ps and 3 ns, respectively, with 532 nm laser-pulse excitation. The spectra recorded at 355 nm laser-pulse excitation are also shown for comparison.

With 532 nm laser-pulse excitation, we observe a red-shifted bleaching with a maximum in the 500−550 nm region. This shows that the clusters that contribute to the surface plasmon band at 420 nm are unaffected by this long-wavelength excitation. Furthermore, we observe a growth of absorption in the 420 and 660 nm region at longer times. The growth rate of the 660 nm transient absorption was comparable to that observed with 355 nm laser-pulse excitation ($\tau = 1.5$ ns). The interesting observation is the growth in the 420 nm region, which we attribute to the fragmentation of larger clusters that selectively absorb 532 nm laser pulse. This situation is similar to the breakup of the silver aggregates observed with 355 nm laser-pulse excitation, but only to a limited extent. Since the particles that contribute to the main plasmon band do not absorb the 532 nm laser pulse, we do not see bleaching at 420 nm. Instead, we observe an increased absorption in this spectral region. Obviously, we create smaller particles that have a plasmon band around 420 nm. The laser-dose dependence of the transient bleach at 520 nm was monophotonic, while the long-term absorption at 660 nm was multiphotonic. This confirms that the photophysical processes observed with 355 and 532 nm laser-pulse excitations are similar. The difference in the

observed transient spectra mainly arises from the fact that different-sized particles are being excited at different pump wavelengths.

Discussion

Nanoparticles of noble metals show photochemical activity when subjected to UV irradiation. For example, they readily undergo photodissolution in the presence of an electron scavenger such as N_2O.[5] The photoemission of electrons into the solvents in such colloidal particles may also be significantly enhanced compared with that in bulk materials because of the lower density of states in the conduction band of the metal nanoparticles. Likewise, Auger scattering processes, which can also lead to electron ejection, should also be enhanced in metal nanoclusters compared with those in bulk metals, since the excited electron−hole pairs are confined to a smaller volume.

The light-induced reactions for Ag nanoclusters in the present experiments are summarized in the following scheme (reactions 1−3).

$$(Ag)_n + 2h\nu \rightarrow (Ag)_n^+ + e_{aq}^- \quad (1)$$

$$(Ag)_n^+ + e_{aq}^- \rightarrow (Ag)_n \quad (2)$$

$$(Ag)_n^+ \rightarrow (Ag)_{n-1} + Ag^+ \quad (3)$$

The photoejection of electrons (reaction 1) is a biphotonic process as observed from the results in Figure 6. This ultrafast process is completed within the laser-pulse duration of 18 ps. Although some of these ejected electrons undergo quick recombination (reaction 2), the rest will accumulate at or near the colloid surface. In the present investigation, we have excluded electron scavengers to minimize the photodissolution effects. The absorption of electrons trapped at the particle surface and/or solvated electrons and also the absorption changes caused by $(Ag)_n^+$ are smaller than the transient absorption/bleach related to the plasmon absorption band. Hence, it is difficult to monitor the dynamics of these species independently.

The electrons that do not undergo photoejection are rapidly thermalized by electron−phonon scattering. The time scale for this process is around 1 ps in bulk metals and is similar for these 50 nm particles.[40] (A detailed investigation of the short-time dynamics in Ag particles will be published elsewhere.) We note here that this decay time is similar to the ∼1ps time for colloidal gold films observed by Feldstein and co-workers.[13] The energy deposited into the phonon modes is subsequently transferred to the surrounding medium on a 10−100 ps time scale.[10] Dumping thermal energy into the solvent causes the dielectric of the surrounding medium to change, which in turn, influences the plasmon resonance frequency of the silver nanoclusters. The bleaching growth component of ∼90 ps observed in the present study probably arises from the heating of the solvent that surrounds the Ag nanoclusters.

The remainder of the dynamics observed in Figure 4 (specifically the 1.5 ns growth component) arises from the electron ejection process, which is predominant at high laser excitation intensities. This process leads to charging of the surface of the 50−60 nm diameter silver nanoclusters. This in turn causes them to disintegrate and form smaller-size particles (5−20 nm diameter). The fact that fragmentation occurs is evident from both the absorption spectra of UV-irradiated samples and the TEM pictures presented in Figures 1 and 2, respectively. A possible reaction scheme leading to the photofragmentation of Ag nanoclusters is shown in Figure 9. Another

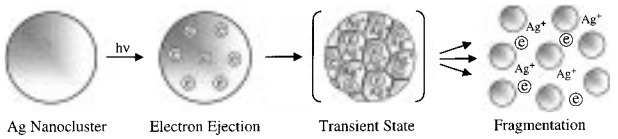

Figure 9. Fragmentation of Ag cluster with laser excitation. A transient aggregate formed via the photoejection of electrons is considered to be a precursor for complete fragmentation of the particle.

possibility is complete dissolution followed by the reduction of Ag^+ ions with aqueous electrons to form smaller particles. However, if this occurred, we would expect to observe a total bleach of the plasmon band followed by a slower diffusion-limited process of cluster formation. The fast bleaching recovery and the transient absorption growth with a time constant of 1.5 ns do not support this possibility. Also, as shown earlier,[5] the dissolution process dominates only when photoejected electrons are scavenged with species such as N_2O. Thus, in the present experiments, instead of complete dissolution, we are fragmenting larger silver nanoclusters into smaller ones using 355 nm laser-pulse excitation. The dissolution of a few surface Ag atoms probably occurs but is not considered significant in the present experiments.

As the larger silver clusters become charged with electrons at their surface, intraparticle changes occur. The broad absorption that is observed in the red region with a 1.5 ns growth component indicates the formation of a transient state, which is an intermediate in the fragmentation process. We interpret this transient to be essentially an aggregate of smaller clusters and trapped electrons that are in proximity. It is well-known that aggregation of small Ag particles leads to a broad plasmon absorption band across the entire visible spectrum.[6] The time constant of 1.5 ns, corresponding to the absorption growth in Figure 4, shows the time frame with which chemical and physical changes occur in the parent Ag cluster following the photoejection of electrons to form the transient intermediate. This transient aggregate then disintegrates and liberates smaller Ag nanoclusters. The 14.2 ns decay component of the transient absorption at 600 nm (Figure 7) corresponds to the time frame with which this ultimate fragmentation occurs. The smaller clusters that are formed from this process are stable and possess properties that are exclusive to smaller-size particles (e.g., exhibiting a 400 nm plasmon band maximum).

By comparing the two power dependencies shown in Figures 5 and 6, we can conclude that the primary event following the laser excitation is the photoexcitation of electrons causing the plasmon absorption to bleach. Comparison of the 175 ps spectrum recorded at lower laser intensity shows plasmon bleach but no noticeable longer-time (3 ns) absorption at similar excitation intensity. The visible absorption only appears at higher laser intensities (>1 mJ/pulse) where a nonlinear process becomes dominant. This visible absorption is not due to solvated electrons or electrons trapped at the metal−liquid interface, since such species should appear instantaneously, that is, within the excitation laser pulse and not with a growth time constant of 1.5 ns. The visible absorption arises from the transient aggregates of 5−20 nm particles that are intermediates in the fragmentation process. These transient aggregates are produced as a result of photoejection of electrons and charging of the particle surface. The photoejection process itself is a multiphotonic process. The 532 or 355 nm laser pulses are not sufficiently energetic to directly (monophotonically) photoeject electrons.[41] Thus, the number of transient aggregates and the magnitude of the visible absorption have a nonlinear dependence on the excitation laser intensity.

Conclusions

The 40−60 nm silver particles produced by the citrate reduction method in aqueous medium undergo fragmentation when subjected to 355 or 532 nm laser-pulse excitation. Selectivity for fragmenting silver clusters into smaller ones can be achieved with the choice of the excitation wavelength. Picosecond pump/probe studies confirm that the electron ejection is one of the primary photochemical events that lead to the photofragmentation process.

Acknowledgment. The work described herein was supported by the Office of the Basic Energy Sciences of the U.S. Department of Energy. This is Contribution No. 4038 from the Notre Dame Radiation Laboratory.

References and Notes

(1) Mulvaney, P. In *Semiconductor Nanoclusters—Physical, Chemical and Catalytic Aspects*; Kamat, P. V., Meisel, D., Eds.; Elsevier Science: Amsterdam, 1997; p 99.
(2) Zhang, J. Z. *Acc. Chem. Res.*, in press.
(3) Sass, J. K.; Sen, R. K.; Meyer, E.; Gerischer, H. *Surf. Sci.* **1974**, *44*, 515.
(4) Mulvaney, P.; Linnert, T.; Henglein, A. *J. Phys. Chem.* **1991**, *95*, 7843.
(5) Linnert, T.; Mulvaney, P.; Henglein, A. *Ber. Bunsen-Ges. Phys. Chem.* **1991**, *95*, 838.
(6) Kreibig, U.; Vollmer, M. *Optical Properties of Metal Clusters*; Springer: Berlin, 1995.
(7) Kreibig, U.; Gartz, M.; Hilger, A.; Hovel, H. In *Fine Particles Science and Technology*; Pelizzatti, E., Ed.; Kluwer Academic Publishers: Boston, 1996; p 499.
(8) Heilweil, E. J.; Hochstrasser, R. M. *J. Chem. Phys.* **1985**, *82*, 179.
(9) Roberti, T. W.; Smith, B. A.; Zhang, J. Z. *J. Chem. Phys.* **1995**, *102*, 3860.
(10) Ahmadi, T. S.; Logunov, S. L.; El-Sayed, M. A. *J. Phys. Chem.* **1996**, *100*, 8053.
(11) Smith, B. A.; Zhang, J. Z.; Giebel, U.; Schmid, G. *Chem. Phys. Lett.* **1997**, *270*, 139.
(12) Jose, H.; Martini, I.; Hartland, G. V. *Chem. Phys. Lett.* **1998**, *284*, 135.
(13) Feldstein, M. J.; Keating, C. D.; Liau, Y.-H.; Natan, M. J.; Scherer, N. F. *J. Am. Chem. Soc.* **1997**, *119*, 6638.
(14) Henglein, A. *J. Phys. Chem.* **1993**, *97*, 5457.
(15) Mulvaney, P.; Giersig, M.; Henglein, A. *J. Phys. Chem.* **1993**, *97*, 7061.
(16) Liz-Marzán, L. M.; Giersig, M.; Mulvaney, P. *Langmuir* **1996**, *12*, 4329.
(17) Haesselbarth, A.; Eychmueller, A.; Eichberger, R.; Giersig, M.; Mews, A.; Weller, H. *J. Phys. Chem.* **1993**, *97*, 5333.
(18) Freeman, R. G.; Hommer, M. B.; Grabar, K. C.; Jackson, M. A.; Natan, M. J. *J. Phys. Chem.* **1996**, *100*, 718.
(19) Martino, A.; Yamanaka, S. A.; Kawola, J. S.; Loy, D. A. *Chem. Mater.* **1997**, *9*, 423.
(20) Hornyak, G. L.; Patrissi, C. J.; Martin, C. R. *J. Phys. Chem. B* **1997**, *101*, 1548.
(21) Shanghavi, B.; Kamat, P. V. *J. Phys. Chem. B* **1997**, *101*, 7675.
(22) Kamat, P. V. In *Semiconductor Nanoclusters—Physical, Chemical and Catalytic Aspects.*; Kamat, P. V., Meisel, D., Eds.; Elsevier Science: Amsterdam, 1997; p 237.
(23) Henglein, A. *Chem. Mater.* **1998**, *10*, 444.
(24) Kraeutler, B.; Bard, A. J. *J. Am. Chem. Soc.* **1978**, *100*, 4317.
(25) Borgarello, E.; Harris, R.; Serpone, N. *Nouv. J. Chim.* **1985**, *9*, 743.
(26) Turkevich, J.; Stevenson, P. L.; Hillier, J. *Discuss. Faraday Soc.* **1951**, *11*, 55.
(27) Ebbesen, T. W. *Rev. Sci. Instrum.* **1988**, *59*, 1307.
(28) Kamat, P. V.; Ebbesen, T. W.; Dimitrijevic, N. M.; Nozik, A. J. *Chem. Phys. Lett.* **1989**, *157*, 384.
(29) Nagarajan, V.; Fessenden, R. W. *J. Phys. Chem.* **1985**, *89*, 2330.
(30) Mulvaney, P.; Henglein, A. *J. Phys. Chem.* **1990**, *94*, 4182.
(31) Linnert, T.; Mulvaney, P.; Henglein, A.; Weller, H. *J. Am. Chem. Soc.* **1990**, *112*, 4657.
(32) Henglein, A.; Holzwarth, A.; Mulvaney, P. *J. Phys. Chem.* **1992**, *96*, 8700.
(33) Mulvaney, P. *Langmuir* **1996**, *12*, 788.
(34) Mie, G. *Ann. Phys. B* **1908**, *25*, 377.
(35) Linnert, T.; Mulvaney, P.; Henglein, A. *J. Phys. Chem.* **1993**, *97*, 679.
(36) Gutierrez, M.; Henglein, A. *J. Phys. Chem.* **1993**, *97*, 11368.
(37) Henglein, A.; Mulvaney, P.; Linnert, T. *Faraday Discuss.* **1991**, *92*, 31.
(38) Persson, B. N. J. *Phys. Rev. B* **1989**, *39*, 8220.
(39) Matsumoto, H.; Sakata, T.; Mori, H.; Yoneyama, Y. *J. Phys. Chem.* **1996**, *100*, 13781.
(40) Jose, H.; Martini, I.; Hartland, G. V.; Kamat, P. V. *J. Phys. Chem.*, submitted for publication.
(41) The work function of Ag is ca. 4.3 eV, which is much greater than the energy of a 355 nm photon (∼3.5 eV).